Features of separatrix regions in magnetic reconnection: Comparison of 2-D particle-in-cell simulations and Cluster observations

Quanming Lu,[1,2] Can Huang,[1] Jinlin Xie,[3] Rongsheng Wang,[1] Mingyu Wu,[1] Andris Vaivads,[4] and Shui Wang[1]

Received 24 May 2010; revised 9 July 2010; accepted 4 August 2010; published 12 November 2010.

[1] In collisionless magnetic reconnection, the in-plane Hall currents are carried mainly by the magnetized electrons. The in-plane Hall currents are directed toward the X line along the magnetic field lines just inside the separatrices and away from the X line along the separatrices. Such a current system leads to the quadrupole out-of-plane magnetic field with the peaks between the regions carrying the in-plane currents. Simultaneously, the electron flow toward the X line along the separatrices causes electron density depletions along the separatrices. In this paper, the features of separatrix regions in magnetic reconnection and the relations between the electron density depletions and the out-of-plane magnetic field are investigated with both two-dimensional particle-in-cell simulations and Cluster observations. We conclude that the electron density depletions are formed because of the magnetic mirror, and they are outside the peaks of the out-of-plane magnetic field. Such a theoretical prediction is confirmed by both simulations and observations.

Citation: Lu, Q., C. Huang, J. Xie, R. Wang, M. Wu, A. Vaivads, and S. Wang (2010), Features of separatrix regions in magnetic reconnection: Comparison of 2-D particle-in-cell simulations and Cluster observations, *J. Geophys. Res.*, *115*, A11208, doi:10.1029/2010JA015713.

1. Introduction

[2] Magnetic reconnection provides a physical mechanism for fast energy conversion from magnetic energy to plasma kinetic energy, which is manifested by plasma heating and jetting in the reconnection outflow regions [*Sweet*, 1958; *Parker*, 1957; *Vasyliunas*, 1975; *Biskamp*, 2000; *Priest and Forbes*, 2000; *Birn et al.*, 2001; *Wang et al.*, 2010a]. Magnetic reconnection is considered to be associated with many bursts in the solar atmosphere [*Giovanelli*, 1946; *Tsuneta et al.*, 1992; *Ulmschneider et al.*, 1991; *Cargill and Klimchuk*, 1997], the Earth's magnetosphere [*Nishida*, 1978; *Hughes*, 1995; *Ge and Russell*, 2006; *Pu et al.*, 2010], and experimental laboratory plasma [*Wesson*, 1997]. Recent studies have shown that collisionless magnetic reconnection has multiscale structures. At scale lengths below the ion inertial length $\lambda_i = c/\omega_{pi}$ (where ω_{pi} is the ion plasma frequency) around the X line, the motions of ions and electrons decouple. The ions become demagnetized while the electrons are magnetized and frozen in the magnetic field lines [*Sonnerup*, 1979; *Birn et al.*, 2001; *Shay et al.*, 2001; *Wang et al.*, 2010b]. The resulting in-plane Hall currents generated from the relative motions between ions and electrons produce a characteristic quadrupole out-of-plane magnetic field structures [*Sonnerup*, 1979; *Nagai et al.*, 2001; *Pritchett*, 2001; *Ma and Bhattacharjee*, 2001; *Rogers et al.*, 2003; *Fu et al.*, 2006]. The reconnection electric field is dominated by the Hall term in the generalized Ohm's law [*Pritchett*, 2001; *Wan and Lapenta*, 2008]. At scale lengths below the electron inertial length $\lambda_e = c/\omega_{pe}$ (where ω_{pe} is the electron plasma frequency) around the X line, even the electrons become demagnetized. The off-diagonal electron pressure term and electron inertial term in the generalized Ohm's law are the main causes of the reconnection electric field around the X line [*Hesse and Winske*, 1998; *Hesse et al.*, 1999, 2002; *Pritchett*, 2001; *Wan and Lapenta*, 2008]. Because the ion inertial length λ_i is much larger than the electron inertial length λ_e, the fast rate of collisionless reconnection is considered to be determined by the ion-scale Hall term in the ion diffusion region [*Birn et al.*, 2001].

[3] In the ion diffusion region, the ions are demagnetized, and the in-plane Hall currents are carried mainly by the magnetized electrons. The electrons move toward the X line along the separatrices because of the effects of the magnetic mirror, and these electrons are accelerated and then directed away from the X line along the magnetic field lines just inside

[1]CAS Key Laboratory of Basic Plasma Physics, School of Earth and Space Sciences, University of Science and Technology of China, Hefei, China.
[2]State Key Laboratory of Space Weather, Chinese Academy of Sciences, Beijing, China.
[3]CAS Key Laboratory of Basic Plasma Physics, School of Physics, University of Science and Technology of China, Hefei, China.
[4]Swedish Institute of Space Physics, Uppsala, Sweden.

Copyright 2010 by the American Geophysical Union.
0148-0227/10/2010JA015713

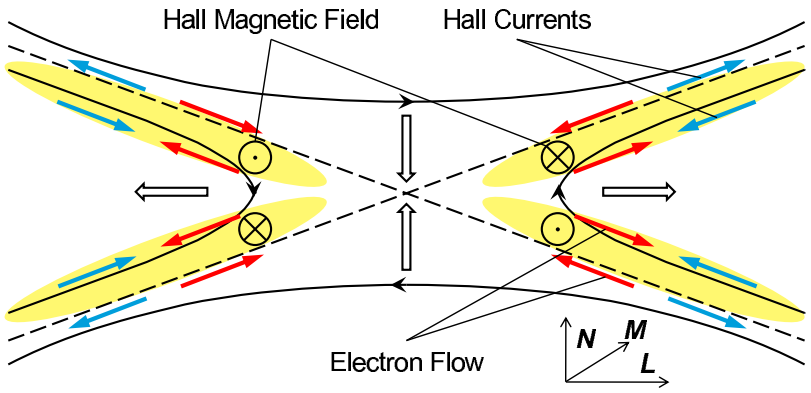

Figure 1. The relations among the Hall currents, out-of-plane magnetic field, and electron density depletions in magnetic reconnection in a current sheet coordinate system: L is along the outflow direction and the N direction is normal to the plane of the neutral sheet. [L, M, N] is a right-handed triplet. The yellow regions denote the out-of-plane magnetic field. The dashed line denotes the separatrix lines, and the electron density depletion layers are along the separatrix lines.

the separatrices after they reach the vicinity of the X line [*Wang et al.*, 2010b]. Therefore, the resulting in-plane Hall currents are directed toward the X line along the magnetic field lines just inside the separatrices and away from the X line along the separatrices [*Nagai et al.*, 2003]. Such a Hall current system leads to the quadrupole out-of-plane magnetic field with the peaks between the regions carrying the in-plane Hall currents [*Birn et al.*, 2001; *Øieroset et al.*, 2001; Nagai et al., 2001; *Pritchett*, 2001; *Ma and Bhattacharjee*, 2001; *Fu et al.*, 2006; *Zhang et al.*, 2008; *Wang et al.*, 2010b]. At the same time, electron density depletions are observed around the separatrix regions [*Øieroset et al.*, 2001; *Vaivads et al.*, 2004; *Cattell et al.*, 2005; *Khotyaintsev et al.*, 2006], and they are found to be along the separatrices [*Mozer et al.*, 2002]. Electron density depletions in magnetic reconnection have also been investigated with particle-in-cell (PIC) simulations [*Drake et al.*, 2005; *Cattell et al.*, 2005], and they are found to be along the separatrices. *Cattell et al.* [2005] further found that in antiparallel reconnection, the structures of electron density depletions are symmetric, while in guide field reconnection, one pair of depletions becomes much deeper than that without a guide field, and the other is filled in. Therefore, we can conclude that in antiparallel reconnection the electron density depletions are outside the peaks of the out-of-plane magnetic field. The relations among the Hall currents, out-of-plane magnetic field, and electron density depletions in antiparallel reconnection are depicted in Figure 1.

[4] On 20 February 2002 around 1300–1400 UT, Cluster observed a reconnection event when crossing the magnetopause, and this event has no obvious global guide field. The same event has already been studied by *Vaivads et al.* [2004], which was used to analyze the electric field around the separatrices. In this paper, we first study the features of separatrix regions with two-dimensional (2-D) particle-in-cell (PIC) simulations, then confirm by Cluster observations the conclusion that the electron density depletions are outside the peaks of the out-of-plane magnetic field.

[5] The paper is organized as follows. The relations between the out-of-plane magnetic field and electron density depletions are investigated with PIC simulations and observations in section 2 and 3, respectively. The conclusions are described in section 4.

2. PIC Simulations of the Out-of-Plane Magnetic Field and Electron Density Depletions

[6] A 2-D PIC simulation code is used in this paper to investigate the relations between the out-of-plane magnetic field and electron density depletions in magnetic reconnection without an initial guide field. In the simulations, the electromagnetic fields are defined on the grids and updated by solving the Maxwell equations with a full explicit algorithm. In our simulation model, the initial configuration is a one-dimensional Harris current sheet in the (x, z) plane, and the initial magnetic field is given by [*Harris*, 1962]

$$\mathbf{B}_0(z) = B_0 \tanh\left(\frac{z}{\delta}\right)\mathbf{e}_x, \tag{1}$$

where δ is the half width of the current sheet. B_0 is the asymptotical magnetic strength. The corresponding number density is

$$n(z) = n_b + n_0 \mathrm{sech}^2\left(\frac{z}{\delta}\right), \tag{2}$$

where n_b represents the density of the background plasma, and n_0 is the peak Harris density. The distribution functions for the ions and electrons are Maxwellian, and their drift speeds in the y direction satisfy $V_{i0}/V_{e0} = T_{i0}/T_{e0}$, where $V_{i0}(V_{e0})$ and $T_{i0}(T_{e0})$ are the drift speed and initial temperature for ions (electrons), respectively. In our simulations, the temperature ratio is $T_{i0}/T_{e0} = 4$, and $n_0 = 5n_b$. The current sheet width is $\delta = 0.5\lambda_i = 0.5c/\omega_{pi}$, where λ_i is the ion inertial length defined by n_0. The mass ratio is set to be $m_i/m_e = 100$. The light speed is $c = 15v_A$, where v_A is the Alfven speed defined by B_0 and n_0.

[7] The computation is carried out in a rectangular domain in the (x, z) plane with dimension $L_x \times L_z = (25.6\lambda_i) \times (12.8\lambda_i)$. An $N_x \times N_z = 512 \times 256$ grid system is employed in the simulations, so the spatial resolution is $\Delta x = \Delta z = 0.05c/\omega_{pi} = 0.5c/\omega_{pe}$. The time step is $\Omega_i t = 0.001$, where Ω_i is the ion

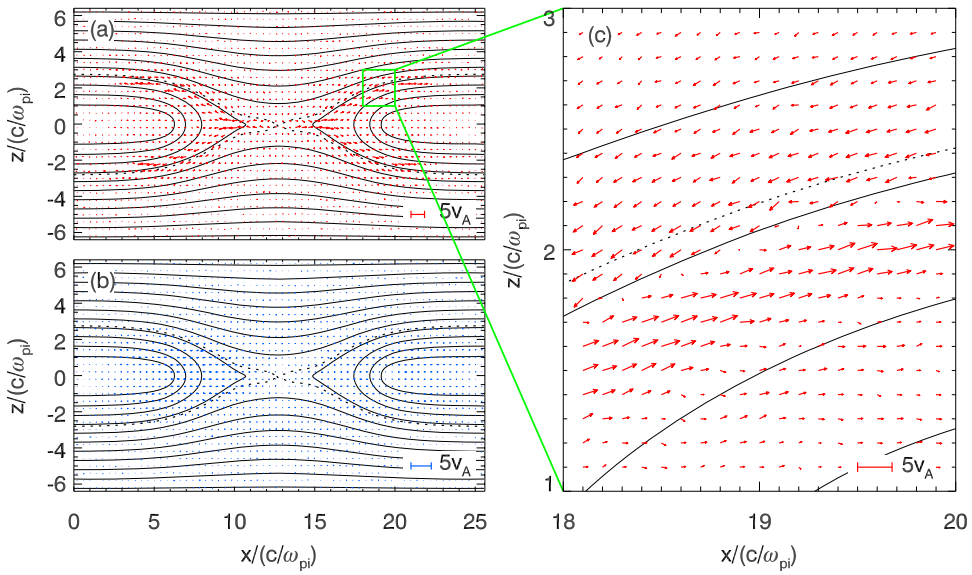

Figure 2. The in-plane (x, z) (a) electron and (b) ion flow velocities at $\Omega_i t = 27$ and (c) the enlarged view of the marked region in Figure 2a. At this time, the reconnection has the maximum reconnection rate.

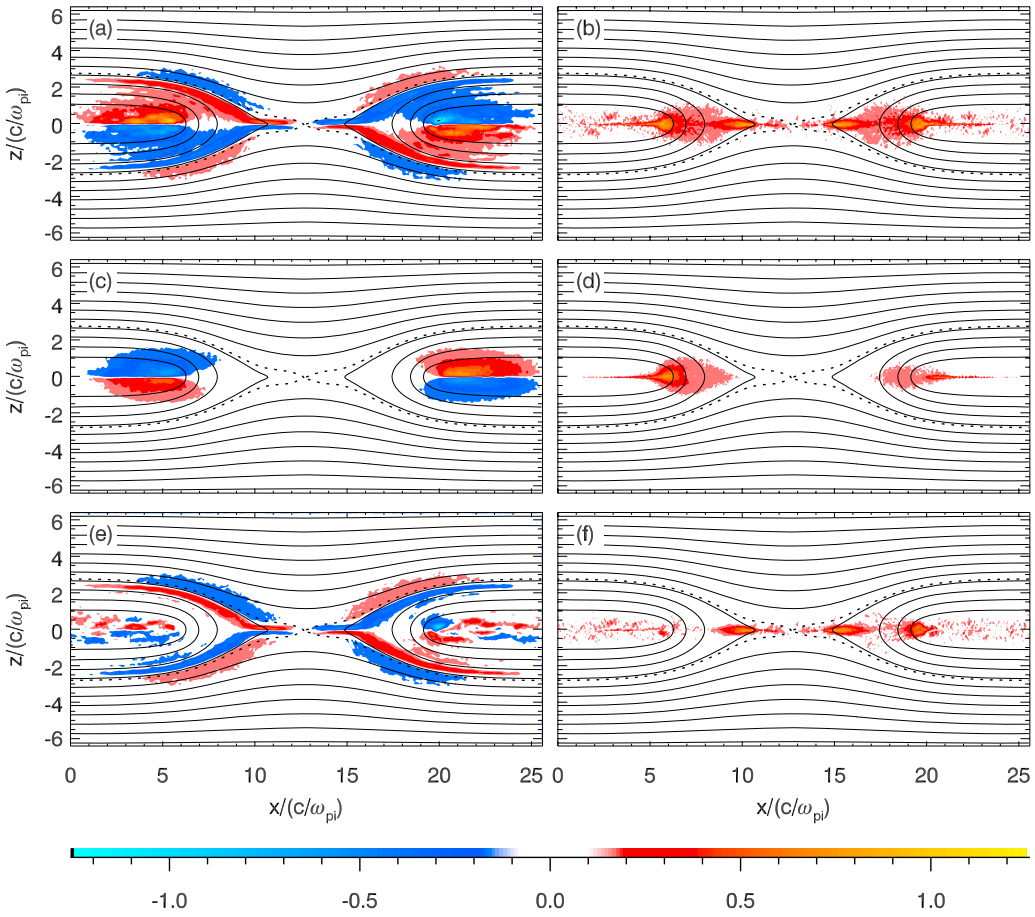

Figure 3. (a) The electron currents along the magnetic field lines $j_{e\|} = \mathbf{J}_e \cdot \mathbf{B}/B$, (b) the electron currents perpendicular to the magnetic field lines $j_{e\perp} = |\mathbf{J}_e - j_{e\|}\mathbf{B}/B|$, (c) the ion currents along the magnetic field lines $j_{i\|} = \mathbf{J}_i \cdot \mathbf{B}/B$, (d) the ion currents perpendicular to the magnetic field lines $j_{i\perp} = |\mathbf{J}_i - j_{i\|}\mathbf{B}/B|$, (e) the total currents along the magnetic field lines $j_{\|} = \mathbf{J} \cdot \mathbf{B}/B$, and (f) the total currents perpendicular to the magnetic field lines $j_{\perp} = |\mathbf{J} - j_{\|}\mathbf{B}/B|$ at $\Omega_i t = 27$.

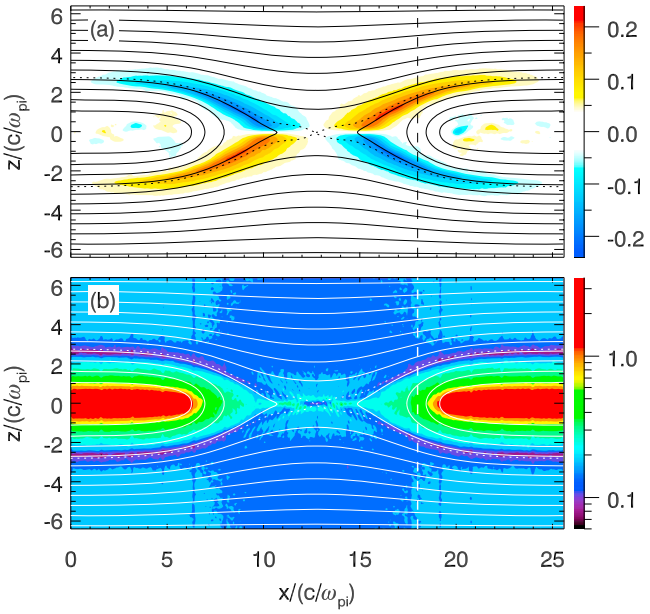

Figure 4. The contours of (a) the out-of-plane magnetic field B_y and (b) the electron density n_e at $\Omega_i t = 27$. The dashed lines denote the position where the profiles are taken in Figure 6.

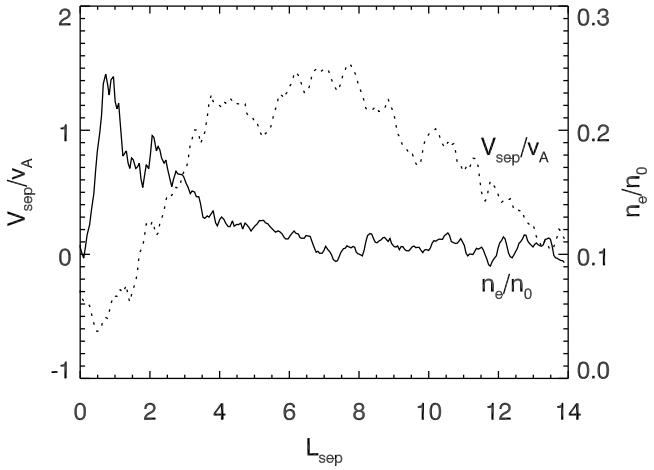

Figure 5. The average electron flow velocity V_{sep} (dotted line) and electron density n_e (solid line) in the direction along the upper right separatrix. The positive velocity means that electrons are directed toward the X line, and the distance is measured from the X line along the upper right separatrix.

gyrofrequency. We employ more than 1.0×10^7 particles per species. The periodic boundary conditions are used along the x direction, while the ideal conducting boundary conditions for electromagnetic fields and reflected boundary conditions for particles are employed in the z direction. In order to make the system enter the nonlinear stage quickly, an initial flux perturbation is introduced, which is useful to reach the stage of rapid growth of reconnection.

[8] Figure 2 shows the in-plane (x, z) electron (Figure 2a) and ion (Figure 2b) flow velocities at $\Omega_i t$ = 27 and the enlarged view of the marked region (Figure 2c). At this time, the reconnection has the maximum reconnection rate. From Figure 2, we can know that the electron flow velocity is much larger than the ion flow velocities. Around the separatrices, ions are unmagnetized, and the ion flow velocity is very small. Electrons are magnetized around the separatrices. As described by *Wang et al.* [2010b], they move toward the X line along the separatrices because of the effects of magnetic mirror and then are accelerated in the vicinity of the X line. At last, they leave the X line along the magnetic field lines just inside the separatrices. Therefore, the in-plane Hall currents around the separatrices are dominated by electron currents. This can be demonstrated in Figure 3, which depicts the electron currents along the magnetic field lines $j_{e\|} = \mathbf{J}_e \cdot \mathbf{B}/B$ (Figure 3a), the electron currents perpendicular to the magnetic field lines $j_{e\perp} = |\mathbf{J}_e - j_{e\|}\mathbf{B}/B|$ (Figure 3b), the ion currents along the magnetic field lines $j_{i\|} = \mathbf{J}_i \cdot \mathbf{B}/B$ (Figure 3c), the ion currents perpendicular to the magnetic field lines $j_{i\perp} = |\mathbf{J}_i - j_{i\|}\mathbf{B}/B|$ (Figure 3d), the total currents along the magnetic field lines $j_{\|} = \mathbf{J} \cdot \mathbf{B}/B$ (Figure 3e), and the total currents perpendicular to the magnetic field lines $j_{\perp} = |\mathbf{J} - j_{\|}\mathbf{B}/B|$ at $\Omega_i t$ = 27 (Figure 3f). For the currents along the magnetic field lines, around the separatrices, the total currents are dominated by the electron currents, and the ion currents are negligible, while in the outflow region, there are no obvious total currents because the electron currents and ion currents are almost cancelled. Therefore, we can observe that the currents are away from the X line along the separatrices and directed toward the X line just inside the separatrices. For the currents perpendicular to the magnetic field lines, all the currents are concentrated in the pileup regions (with large ∇B).

[9] Figure 4 shows the contours of the out-of-plane magnetic field B_y (Figure 4a) and the electron density n_e at $\Omega_i t$ = 27 (Figure 4b). The out-of-plane magnetic field B_y exhibits a quadrupole structure, and there are depletions in the electron density along the separatrices. The regions with maximum B_y lie inside the regions of electron density depletion at the separatrices. Electron density depletions along the separatrices can be explained on the basis of Figure 5, which describes the average electron flow velocity

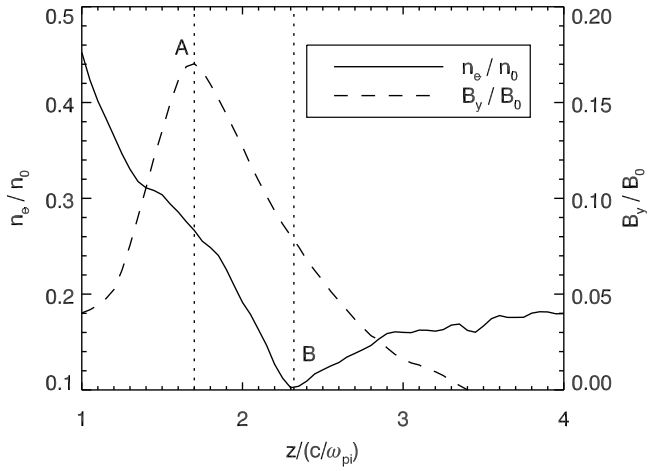

Figure 6. The profiles of the out-of-plane magnetic field B_y and the electron density n_e along $x = 18c/\omega_{pi}$. The dotted lines denote the positions with the maximum B_y and the minimal electron density.

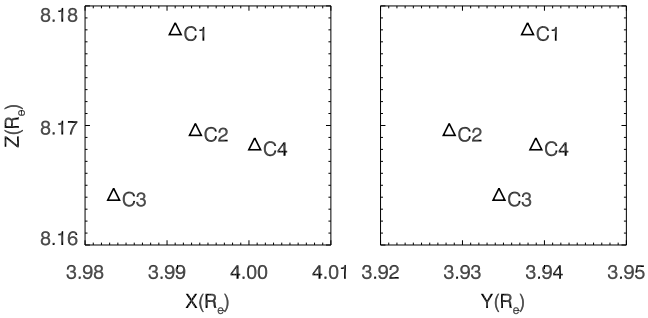

Figure 7. The location of Cluster at 1320 UT on 20 February 2002 in the GSE coordinates.

V_{sep} and electron density n_e in the direction along the upper right separatrix. In Figure 5, the positive velocity means that electrons are directed toward the X line. Obviously, in the regions except the vicinity of the X line, average electron flow velocities in the direction along the separatrices increase as electrons approach the X line, while electron densities almost do not change. Therefore, the net mass flux in any small region along the separatrices is negative. This leads to the decrease in electron density that forms electron density depletion layers. The relation between the out-of-plane magnetic field and electron density depletion can be demonstrated more clearly in Figure 6, which shows the profiles of the out-of-plane magnetic field B_y and the electron density n_e along $x = 18c/\omega_{pi}$. The minimal value of the electron density is about $n_e = 0.1n_0$, and its position is about $z = 2.3c/\omega_{pi}$. The maximum value of the out-of-plane magnetic field B_y is about $B_y = 0.17B_0$, and its position is about $z = 1.7c/\omega_{pi}$. Obviously, the position with the maximum B_y is inside that with the minimal electron density (the electron density depletion), and their difference is about $z = 0.6c/\omega_{pi}$.

3. Cluster Observations of the Out-of-Plane Magnetic Field and Electron Density Depletions

[10] On 20 February 2002 around 1300–1400 UT, Cluster observed a reconnection event when crossing the Earth's magnetopause many times tailward and duskward of the cusp. The separation between the spacecraft is about 100 km which is comparable to the ion inertial length $\lambda_i = c/\omega_{pi}$ = 75 km. This event does not have an obvious global guide field and is almost symmetric. Figure 7 shows the location of Cluster at 1320 UT on 20 February 2002 in the GSE coordinates. Cluster was located around $X = 4$, $Y = 4$, and $Z = 8$ R_E (R_E is the Earth's radius). C1 was the northernmost spacecraft, while C3 was the southernmost spacecraft. Magnetic field data are taken from the fluxgate magnetometer (FGM) [*Balogh et al.*, 2001], which measures the three components of the low-frequency magnetic field. The electron density is obtained from the spacecraft potential measurements of the Electric Field and Wave (EFW) experiment [*Gustafsson et al.*, 2001; *Pedersen et al.*, 2008].

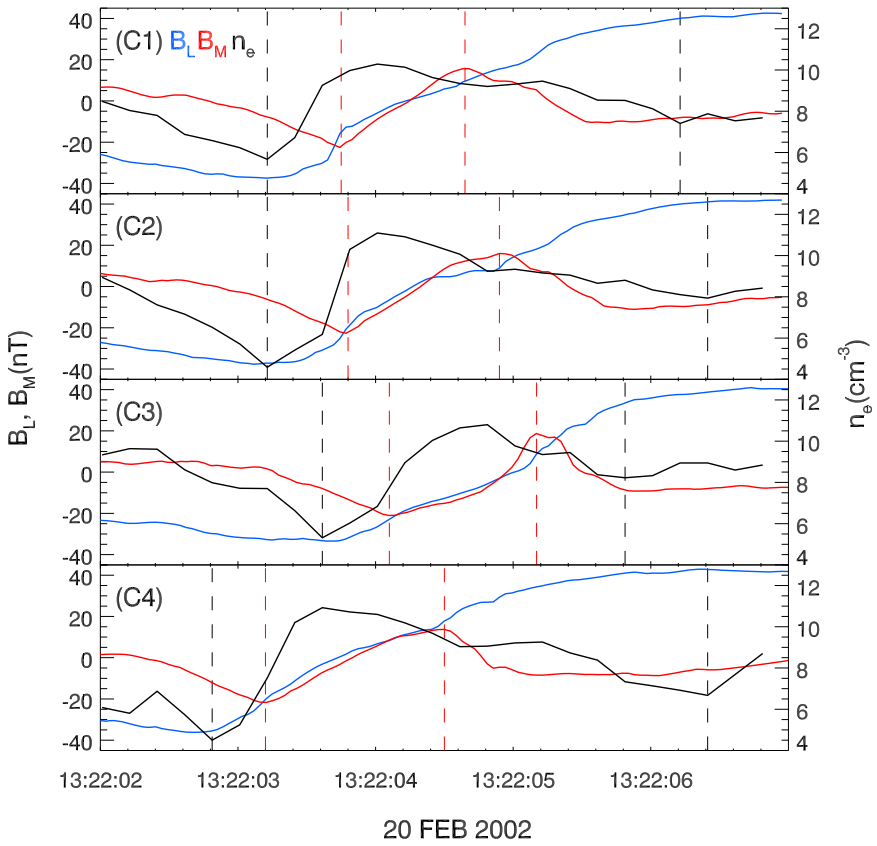

Figure 8. B_L, B_M, and the electron density n_e for C1, C2, C3, and C4 during the interval 1322:02–1322:07 UT. The data are shown in a current sheet coordinate system. The time resolution of the electron density is 0.2 s; the others are 1/22 s.

[11] Figure 8 shows Cluster observations of B_L, B_M, and the electron density n_e for C1, C2, C3, and C4 during the interval 1322:02–1322:07 UT. The data are shown in a current sheet coordinate system: L is along the outflow direction, and the N direction is normal to the plane of the neutral sheet. [L, M, N] is a right-handed triplet. L = [−0.17, 0.53, 0.83], M = [0.54, −0.65, 0.53], and N = [0.82, 0.54, −0.18] in the GSE coordinate system. B_L, B_M are components of the magnetic field in the L and M directions, respectively. The time resolution of the electron density is 0.2 s; the others are 1/22 s. This reconnection event has already been investigated by *Vaivads et al.* [2004]. During this interval, Cluster crosses the current sheet rapidly, and the out-of-plane magnetic field B_M shows a bipolar structure. We can also find that there are electron density depletions at the edges of the current sheet, and the locations with the minimal values of the electron density n_e correspond to larger amplitude of B_L than that with the maximum values of the out-of-plane magnetic field B_M. At the lower edge of the current sheet, the values of B_L corresponding to the minimal values of the electron density n_e are about −37 nT, −37 nT, −33 nT, and −36 nT for C1, C2, C3, and C4, respectively, while the values of B_L corresponding to the maximum values of B_M are about −16 nT, −21 nT, −23 nT, and −20 nT for C1, C2, C3, and C4, respectively. At the upper edge of the current sheet, the values of B_L corresponding to the minimal values of the electron density n_e are about 39 nT, 41 nT, 31 nT, and 43 nT for C1, C2, C3, and C4, respectively, while the values of B_L corresponding to the maximum values of B_M are about 10 nT, 9 nT, 9 nT, and 18 nT for C1, C2, C3, and C4, respectively. Therefore, the position with the maximum values of B_M is inside the position with the minimal values of the electron density n_e (the electron density depletion). In addition, according to the separation of the spacecraft and the time delay between the current sheet crossing (B_L = 0), the moving velocity of the current sheet along the N direction can be calculated to be 120 km/s in the (L, M, N) coordinate. The time differences between the maximum values of B_M and the minimal values of n_e are 0.4–0.6 s at the lower edge and 0.6–1.8 s at the upper edge of the current. The separations between the maximum values of B_M and the minimal values of n_e are 48–72 km at the lower edge and 72–216 km at the upper edge of the current sheet, which is 0.64–2.9λ_i. This is consistent with the simulation, where the separations between the maximum values of B_M and the minimal values of n_e are about 0.6λ_i.

4. Conclusions

[12] The in-plane Hall currents play a key role of dissipation in collisionless magnetic reconnection. The characteristic quadrupole out-of-plane magnetic field structures are considered to be the evidence for the existence of the in-plane Hall currents [*Birn et al.*, 2001; *Øieroset et al.*, 2001]. In this paper, we study the features of separatrix regions in magnetic reconnection by comparing 2-D PIC simulations and Cluster observations. The electron density depletions are found to be along the separatrices, and they are outside the peaks of the out-of-plane magnetic field. In addition, from both simulations and observations, their separations between the electron density depletions and the peaks of the out-of-plane magnetic field are found to be around the ion inertial length. This gives further evidence of the in-plane Hall currents.

[13] **Acknowledgments.** This research was supported by the National Science Foundation of China (NSFC) under grants 40725013, 4097401, 40931053, Chinese Academy of Sciences grant KJCX2-YW-N28, and the Specialized Research Fund for State Key Laboratories. All Cluster data are obtained from the ESA Cluster Active Archive. We thank the FGM and EFW instrument teams and ESA Cluster Active Archive.

[14] Philippa Browning thanks David Sibeck and another reviewer for their assistance in evaluating this paper.

References

Balogh, A., et al. (2001), The Cluster magnetic field investigation: Overview of in-flight performance and initial results, *Ann. Geophys.*, *19*, 1207.

Birn, J., et al. (2001), Geospace Environmental Modeling (GEM) Magnetic Reconnection Challenge, *J. Geophys. Res.*, *106*, 3715.

Biskamp, D. (2000), *Magnetic Reconnection in Plasmas*, Cambridge Univ. Press, Cambridge, U. K.

Cargill, P. A., and J. A. Klimchuk (1997), A nanoflare explanation for the heating of coronal loops observed by *Yohkoh*, *Astrophys. J.*, *478*, 799.

Cattell, C., et al. (2005), Cluster observations of electron holes in association with magnetotail reconnection and comparison to simulations, *J. Geophys. Res.*, *110*, A01211, doi:10.1029/2004JA010519.

Drake, J. F., M. A. Shay, W. Thongthai, and M. Swisdak (2005), Production of energetic electrons during magnetic reconnection, *Phys. Rev. Lett.*, *94*, doi:10.1103/PhysRevLett.94.095001.

Fu, X. R., Q. M. Lu, and S. Wang (2006), The process of electron acceleration during collisionless magnetic reconnection, *Phys. Plasmas*, *13*, 012309, doi:10.1063/1.2164808.

Ge, Y. S., and C. T. Russell (2006), Polar survey of magnetic field in near tail: Reconnection rare inside 9 R_E, *Geophys. Res. Lett.*, *33*, L02101, doi:10.1029/2005GL024574.

Giovanelli, R. G. (1946), A theory of chromospheric flares, *Nature*, *158*, 81.

Gustafsson, G., et al. (2001), First results of electric field and density observations by Cluster EFW based on initial months of operation, *Ann. Geophys.*, *19*, 1219.

Harris, E. G. (1962), On a plasma sheath separating regions of oppositely directed magnetic field, *Nuovo Cimento Soc. Ital. Fis.*, *23*, 115.

Hesse, M., and D. Winske (1998), Electron dissipation in collisionless magnetic reconnection, *J. Geophys. Res.*, *103*, 26,479.

Hesse, M., K. Schindler, J. Birn, and M. Kuznetsova (1999), The diffusion region in collisionless magnetic reconnection, *Phys. Plasmas*, *6*, 1781.

Hesse, M., M. Kuznetsova, and M. Hoshino (2002), The structure of the dissipation region for component reconnection: Particle simulations, *Geophys. Res. Lett.*, *29*(12), 1563, doi:10.1029/2001GL014714.

Hughes, W. J. (1995), *Introduction to Space Physics*, edited by M. G. Kivelson and C. T. Russell, p. 227, Cambridge Univ. Press, New York.

Khotyaintsev, Y. V., A. Vaivads, A. Retino, M. Andre, C. J. Owen, and N. Nilsson (2006), Formation of inner structure of a reconnection separatrix region, *Phys. Rev. Lett.*, *97*, doi:10.1103/PhysRevLett.97.205003.

Ma, Z. W., and A. Bhattacharjee (2001), Hall magnetohydrodynamic reconnection: The Geospace Environment Modeling challenge, *J. Geophys. Res.*, *106*, 3773.

Mozer, F. S., S. D. Bale, and T. D. Phan (2002), Evidence of diffusion regions at a subsolar magnetopause crossing, *Phys. Rev. Lett.*, *89*, 015002, doi:10.1103/PhysRevLett.89.015002.

Nagai, T., I. Shinohara, M. Fujimoto, M. Hoshino, Y. Saito, S. Machida, and T. Mukai (2001), Geotail observations of the Hall current system: Evidence of magnetic reconnection in the magnetotail, *J. Geophys. Res.*, *106*, 25,929.

Nagai, T., I. Shinohara, M. Fujimoto, S. Machida, R. Nakamura, Y. Saito, and T. Mukai (2003), Structure of the Hall current system in the vicinity of the magnetic reconnection site, *J. Geophys. Res.*, *108*(A10), 1357, doi:10.1029/2003JA009900.

Nishida, A. (1978), *Geomagnetic Diagnostics of the Magnetosphere*, Springer, New York.

Øieroset, M., T. D. Phan, M. Fujimoto, R. P. Lin, and R. P. Lepping (2001), In situ detection of collisionless reconnection in the Earth's magnetotail, *Nature*, *412*, 414.

Parker, E. N. (1957), Sweet's mechanism for merging magnetic fields in conducting fluid, *J. Geophys. Res.*, *62*, 509.

Pedersen, A., et al. (2008), Electron density estimations derived from spacecraft potential measurements on Cluster in tenuous plasma regions, *J. Geophys. Res.*, *113*, A07S33, doi:10.1029/2007JA012636.

Priest, E., and T. Forbes (2000), *Magnetic Reconnection: MHD Theory and Applications*, Cambridge Univ. Press, Cambridge, U. K.

Pritchett, P. L. (2001), Geospace Environment Modeling magnetic reconnection challenge: Simulations with a full particle electromagnetic code, *J. Geophys. Res.*, *106*, 3783.

Pu, Z. Y., et al. (2010), THEMIS observations of substorms on 26 February 2008 initiated by magnetotail reconnection, *J. Geophys. Res.*, *115*, A02212, doi:10.1029/2009JA014217.

Rogers, B. N., R. E. Denton, and J. F. Drake (2003), Signatures of collisionless magnetic reconnection, *J. Geophys. Res.*, *108*(A3), 1111, doi:10.1029/2002JA009699.

Shay, M. A., J. F. Drake, B. N. Rogers, and R. E. Denton (2001), Alfvénic collisionless magnetic reconnection and the Hall term, *J. Geophys. Res.*, *106*, 3759.

Sonnerup, B. U. Ö. (1979), Magnetic field reconnection, in *Solar System Plasma Physics*, vol. 3, edited by L. J. Lanzèerotti, C. F. Kennel, and E. N. Parker, p. 46, North-Holland, New York.

Sweet, P. A. (1958), *Electromagnetic Phenomena in Cosmical Physics*, edited by B. Lehnert, p. 123, Cambridge Univ. Press, London.

Tsuneta, S., H. Hara, T. Shimizu, L. W. Acton, K. T. Strong, H. S. Hudson, and Y. Ogawara (1992), Observation of a solar flare at the limb with the Yohkoh Soft X-ray Telescope, *Publ. Astron. Soc. Jpn.*, *44*, L63.

Ulmschneider, P., E. R. Priest, and R. Rosner (1991), *Mechanisms of Chromospheric and Coronal Heating*, edited by R. Rosner, Springer, Berlin.

Vaivads, A., Y. Khotyaintsev, M. André, A. Retinò, S. C. Buchert, B. N. Rogers, P. Décréau, G. Paschmann, and T. D. Phan (2004), Structure of the magnetic reconnection diffusion region from four-spacecraft observations, *Phys. Rev. Lett.*, *93*, doi:10.1103/PhysRevLett.93.105001.

Vasyliunas, V. M. (1975), Theoretical models of magnetic field line merging, *Rev. Geophys.*, *13*, 303.

Wan, W. G., and G. Lapenta (2008), Electron self-reinforcing process of magnetic reconnection, *Phys. Rev. Lett.*, *101*, doi:10.1103/PhysRevLett.101.015001.

Wang, R. S., Q. M. Lu, A. M. Du, and S. Wang (2010a), In situ observations of a secondary magnetic island in ion diffusion region and associated energetic electrons, *Phys. Rev. Lett.*, *104*, 175003.

Wang, R. S., Q. M. Lu, C. Huang, and S. Wang (2010b), Multispacecraft observation of electron pitch angle distributions in magnetotail reconnection, *J. Geophys. Res.*, *115*, A01209, doi:10.1029/2009JA014553.

Wesson, J. (1997), *Tokomaks*, Oxford Univ. Press, New York.

Zhang, H., Q. G. Zong, T. A. Fritz, S. Y. Fu, S. Schaefer, K. H. Glassmeier, P. W. Daly, H. Rème, and A. Balogh (2008), Cluster observations of collisionless Hall reconnection at high-latitude magnetopause, *J. Geophys. Res.*, *113*, A03204, doi:10.1029/2007JA012769.

C. Huang, Q. Lu, R. Wang, S. Wang, and M. Wu, CAS Key Laboratory of Basic Plasma Physics, School of Earth and Space Sciences, University of Science and Technology of China, Hefei, Anhui 230026, China. (qmlu@ustc.edu.cn)

A. Vaivads, Swedish Institute of Space Physics, Uppsala SE-75121, Sweden.

J. Xie, CAS Key Laboratory of Basic Plasma Physics, School of Physics, University of Science and Technology of China, Hefei, Anhui 230026, China.